INTERNATIONAL JOURNAL OF INTEGRATED ENGINEERING
ISSN: 2229-838X e-ISSN: 2600-7916

IJIE

Vol. 17 No. 8 (2025) 213-226
https://publisher.uthm.edu.my/ojs/index.php/ijie

Computational Fluid Dynamics Analysis of Substrate Surface Energy and Ink Surface Tension Effects on Deposition of Conductive Ink

Muhammad Nauman Salik[1], Loo Yuen Hern[1], Rd. Khairilhijra' Khirotdin[1]*, Nurhaffizah Hassan[1], Muhamad Syarifuddin Mohd. Yasin[2]

[1] *Faculty of Mechanical and Manufacturing Engineering, Universiti Tun Hussein Onn Malaysia, Parit Raja, Batu Pahat, Johor, 86400, MALAYSIA*
[2] *Dewa Master Resources, No. 13 & 13-1, Jalan Universiti 1, Taman Universiti, Parit Raja, Batu Pahat, Johor, 86400, MALAYSIA*

*Corresponding Author: khairil@uthm.edu.my
DOI: https://doi.org/10.30880/ijie.2025.17.08.019

Article Info

Received: 12 September 2025
Accepted: 9 December 2025
Available online: 31 December 2025

Keywords

Printed electronics, computational fluid dynamics, conductive inks, substrate surface energy, substrate surface tension, line width

Abstract

Precise control of conductive ink deposition remains challenging in printed electronics manufacturing, where substrate variability significantly impacts pattern fidelity and electrical performance. This investigation comprehensively examines how substrate surface energy (SSE) and ink surface tension (ST) interactions govern the formation of line width through integrated computational-experimental methodology. Using Ansys Fluent with enhanced Volume of Fluid modelling, seventeen substrate materials covering surface energies from 16.49 to 65.39 mJ/m^2 were analysed to establish quantitative deposition relationships. The computational framework incorporated a modified formulation accounting for contact angle dynamics and substrate-specific wetting behaviour. Silver conductive ink particles were deposited via controlled droplet methodology to isolate surface energy effects from dispensing variables. Results demonstrate 87.9% variation in line width across the investigated spectrum, with optimal deposition occurring within a narrow SSE range of 40-45 mJ/m^2. FR4 substrates achieved target line widths with minimal deviation (+2.3%), while ceramic materials exceeded targets by up to 53.8%. The enhanced model exhibited a substantial reduction in prediction error compared to conventional approaches, particularly within the optimal surface energy window, where errors remained below 6%. These findings provide manufacturers with actionable guidelines for substrate selection and surface treatment optimization, challenging current quality control paradigms while offering pathways toward more predictable, sustainable manufacturing processes in aerospace structural health monitoring and precision electronics applications.

1. Introduction

The field of printed electronics has revolutionized modern manufacturing by enabling flexible, lightweight, and cost-effective electronic devices through additive deposition techniques. Unlike conventional subtractive methods such as photolithography, printed electronics employ conductive inks to directly pattern substrates, minimizing material waste and production time [1], [2]. Advances in nanomaterial-based inks (such as graphene and silver

nanoparticles) have further enhanced electrical conductivity and mechanical resilience, making them indispensable for applications like embedded structural health monitoring (SHM) sensors in aerospace composites [3], [4]. However, achieving consistent deposition quality remains a critical challenge, primarily due to the complex interplay between substrate surface energy (SSE) and ink surface tension (ST), which governs adhesion, spreading dynamics, and pattern fidelity [5].

A major chall enge in printed electronics stems from substrate variability. High SSE surfaces typically enhance ink adhesion and result in broader, more uniform line widths, whereas low SSE materials often produce narrow, discontinuous lines that compromise electrical performance [6]. Ink rheology adds further complexity because high-viscosity formulations limit spreading, creating thinner traces, while low-viscosity inks can overspread, reducing resolution and causing pattern distortion [7]. Although computational fluid dynamics (CFD) has emerged as a valuable tool for simulating deposition behaviour, current models often oversimplify these interactions, leading to significant discrepancies between simulated and experimental outcomes [2], [8]. Resolving these limitations is critical. It enables the advancement of high-precision applications, such as real-time SHM systems in aerospace, where sensor performance depends on uniform, defect-free deposition.

Despite notable progress in deposition methodologies, unresolved issues remain. Conventional CFD frameworks often overlook dynamic ink–substrate interactions, including shear-thinning effects in high-viscosity inks and SSE variations introduced by surface treatments [5], [6]. Moreover, the interplay between ink ST and substrate wettability, particularly on rough or porous surfaces, remains insufficiently quantified, resulting in suboptimal deposition in demanding operational environments [7]. Aerospace applications amplify these challenges because substrates must simultaneously ensure ink compatibility and withstand stringent thermal and mechanical constraints [8]. Furthermore, while printed SHM sensors such as MXene-based designs demonstrate superior strain sensitivity compared to traditional piezoelectric counterparts, their operational reliability is frequently compromised by deposition inconsistencies and environmental factors such as thermal cycling [9], [10].

The fundamental role of SSE in governing conductive ink deposition behaviour represents a critical yet underexplored aspect of printed electronics manufacturing. SSE defines the thermodynamic energy associated with creating solid-vapor interfaces, establishing whether deposited ink droplets will exhibit beading, complete spreading, or intermediate wetting characteristics on a given substrate. Materials exhibiting high SSE values, including glass and plasma-modified polymer surfaces, typically facilitate enhanced ink-substrate interactions, yielding broader line formations with improved adhesion properties. Conversely, substrates characterized by low SSE, such as untreated thermoplastics and silicone-based materials, frequently result in restricted spreading patterns and discontinuous conductive pathways due to inadequate wetting behaviour [6], [7].

The significance of these phenomena extends beyond laboratory observations, particularly in aerospace SHM, where sensor reliability depends heavily on consistent ink deposition patterns across diverse substrate materials [9], [11]. Given the aerospace industry's increasing adoption of advanced composite materials and flexible substrate technologies, the challenge of maintaining uniform ink behaviour across varying surface energy conditions has emerged as a critical manufacturing consideration requiring systematic investigation through both computational modelling and empirical validation approaches [2]. To overcome these limitations, this research pursues two key objectives: (i) quantifying the influence of SSE and ST on conductive ink line width and deposition accuracy, and (ii) enhancing deposition predictability by integrating SSE and ST dynamics into an Ansys Fluent-based simulation framework. By closing the gap between theory and simulation, this work advances conductive ink deposition for next-generation SHM sensors, ensuring their performance under operational demands.

The present study approaches these challenges through a combined computational and experimental methodology that systematically investigates the effects of SSE and ST on ink deposition. A refined CFD model, implemented within Ansys Fluent and derived from a mathematical framework that incorporates critical parameters such as static contact angle and the Ohnesorge number, was employed to improve the accuracy of ink–substrate interaction predictions [9]. While dispense printing, profilometry, and optical microscopy are identified as suitable techniques for assessing deposition quality on selected substrates, the present work remains focused on simulation to establish the governing influence of interfacial parameters. Model reliability is therefore demonstrated through consistency with established wetting trends in literature, ensuring that the predicted spreading behaviour reflects realistic physical outcomes. A subsequent phase of this research will integrate experimental measurements with profilometry and microscopy to enable direct statistical comparison, including the use of error bars, RMSE, and R^2, thereby strengthening the quantitative basis for predictive capability and supporting scalable manufacturing of printed electronic components tailored for aerospace SHM applications.

Int. Journal of Integrated Engineering Vol. 17 No. 8 (2025) p. 209-226

2. Methodology

2.1 Computational Framework and Simulation Environment

The numerical investigation of conductive ink deposition performance was conducted using Ansys Fluent 2023 R2, employing a comprehensive three-dimensional transient simulation approach. This CFD framework was specifically configured to analyse the influence of SSE and corresponding contact angles on line width formation during the deposition process. The simulation environment incorporated multiphase flow modelling capabilities to capture the complex interaction dynamics between the silver-based conductive ink and various substrate materials. The computational domain utilized an axisymmetric configuration to optimize computational efficiency while maintaining physical accuracy. This approach reduced the overall mesh complexity without compromising the resolution of critical flow phenomena near the droplet-substrate interface. Domain boundaries were positioned sufficiently distant from the deposition zone to prevent artificial boundary effects from influencing the ink spreading behaviour.

2.2 Material Properties and Ink Characterization

The conductive ink formulation utilized throughout the simulation study consisted of a silver particle suspension with carefully characterized material properties. The ink density was specified as 1630 kg/m^3, corresponding to a high-loading silver formulation typical of industrial conductive ink applications. Viscosity measurements established the ink's dynamic viscosity at 2.4 kg/ms under room temperature conditions, positioning it within the optimal range for precision dispensing applications, as can be seen in Fig. 1.

ST constitutes a critical parameter governing droplet formation, stability, and wetting behaviour on the substrate. In this study, an ST value of 0.035 N/m was implemented through Fluent's material property database to accurately capture capillary effects that influence droplet morphology during deposition. Variations in ST significantly affect printed feature quality; higher ST values generally restrict lateral spreading, producing narrower and well-defined conductive paths, whereas lower ST values promote excessive spreading, resulting in wider and less precise patterns. Maintaining an appropriate correlation between SSE and ST is imperative. This prevents characteristic defects, such as edge irregularities, droplet disintegration, and secondary droplet formation. Even minimal deviations in these interfacial properties can adversely impact the functional performance of miniaturized electronic architectures [2]. Industrial strategies to mitigate these effects typically involve substrate surface modification and the incorporation of targeted additives within the ink formulation to enhance interfacial compatibility.

All simulations operated under standard room temperature and pressure (RTP) conditions, specifically 25°C and 101.325 kPa. These environmental parameters remained constant throughout the simulation matrix to isolate the effects of substrate surface properties on deposition outcomes.

Fig. 1 *Input parameters for density and viscosity in Ansys Fluent*

2.3 Multiphase Modelling Approach

The computational framework utilized in this investigation employed the VOF method, which provides excellent capabilities for tracking multiphase interface evolution during conductive ink deposition processes. The VOF method solves momentum equations across the entire computational domain while monitoring volume fractions for each phase, delivering computational efficiency and maintaining interface integrity without requiring excessive processing resources [5]. This technique proves particularly effective for analysing free-surface deformation and ST-driven spreading phenomena, both fundamental characteristics of droplet-substrate interactions in conductive ink applications. Alternative approaches, such as the Level Set method, provide smooth interface tracking capabilities but typically encounter mass conservation difficulties when handling large deformation scenarios. Lagrangian-based and particle-based methods, while offering accuracy for individual droplet modelling, require significant computational resources and become impractical for comprehensive substrate parameter investigations [8].

In broader multiphase modelling practice, several other interface tracking techniques have been proposed, but each presents trade-offs that limit their suitability for printed electronics. The Level Set (LS) method is recognized for its geometric accuracy and smooth curvature calculation, yet it suffers from severe mass loss due to numerical dissipation under coarse resolutions, making it unreliable for predicting droplet spreading volumes [12]. Hybrid schemes such as the coupled Level Set and VOF (CLSVOF) or particle Level Set (PLS) improve mass conservation by combining the strengths of both methods, though at the expense of computational efficiency and algorithmic simplicity, especially on unstructured grids [12], [13]. Phase-Field models provide a diffuse-interface description and capture complex phenomena such as moving contact lines and droplet breakup; however, they require very fine mesh resolution across the transition zone and high computational cost, limiting their practicality for engineering-scale deposition studies [14]. In contrast, the VOF framework achieves robust mass conservation while capturing capillary-driven dynamics with sufficient accuracy at a manageable computational cost, making it the most appropriate choice for simulating conductive ink deposition on varied substrates [13]. A concise comparison of these approaches is presented in Table 1, highlighting their respective strengths, limitations, and applicability to printed electronics.

Table 1 *Comparison of common interface-tracking methods for multiphase CFD*

Method	Strengths	Weaknesses	Suitability for printed electronics	References
VOF	Excellent mass conservation; efficient; widely implemented in commercial solvers.	Curvature estimation is less accurate than LS; it requires reconstruction algorithms.	Well-suited for droplet spreading and substrate wetting at a practical cost.	[13]
Level-set (LS)	Smooth interface representation; accurate curvature and normal calculation.	Prone to numerical dissipation, poor mass conservation, and volume loss in large deformations.	Risk of inaccurate droplet volume retention.	[12], [13]
CLSVOF / PLS (hybrid)	Combines LS accuracy with VOF conservation; good handling of topology changes.	Complex implementation; computationally expensive; limited robustness on unstructured grids.	Accurate but impractical for wide parameter studies.	[12], [13]
Phase-field (diffuse interface)	Physically consistent; captures moving contact lines and breakup; avoids explicit interface reconstruction.	Requires fine resolution; computationally intensive; sensitive to parameter tuning.	More suitable for fundamental studies than applied inkjet simulations.	[13], [14]

The current simulation framework acknowledges that computational models necessarily simplify real-world manufacturing conditions. Several factors, including nozzle ejection dynamics, ink evaporation effects, transient contact angle hysteresis, and substrate surface micro-roughness, were deliberately excluded to minimize model complexity and concentrate specifically on substrate surface energy influences. The implementation of a static, gravity-driven droplet approach rather than a complete jetting simulation was designed to isolate spreading behaviour controlled primarily by interfacial forces. While these modelling simplifications may introduce minor differences between simulated and experimental line width measurements or droplet contact patterns, they do not affect the model's ability to capture essential physics governing material compatibility and wetting characteristics [2], [6]. Consequently, the simulation results provide reliable approximations of ink-substrate interaction behaviour and establish a solid foundation for process parameter optimization in printed electronics and structural health monitoring applications.

Comparable simplifications have been reported in recent literature, where models prioritized substrate ink interactions over complete jetting dynamics. For instance, Pooja et al. [15] focused on equilibrium wetting morphologies on patterned substrates by adopting experimentally derived advancing, receding, and dynamic contact angles as boundary conditions, while deliberately limiting consideration of inertia-dominated impact phases that only persist over microsecond timescales. Their findings emphasize that the late-stage droplet spreading and equilibrium morphology, rather than the transient ejection dynamics, govern the final printed dimensions. Similarly, the numerical framework presented by Pooja et al. [15] modelled droplet motion and

Int. Journal of Integrated Engineering Vol. 17 No. 8 (2025) p. 209-226

spreading on flat surfaces without explicit evaporation terms or nozzle actuation, showing that reliable predictions can still be achieved when the analysis is constrained to spreading under controlled ambient conditions. Drawing on these precedents, the current study isolates substrate surface energy and ink surface tension as the dominant factors influencing deposition outcomes, with the excluded dynamics expected to exert only a secondary influence under the quasi-static, syringe-based dispensing conditions employed.

2.4 Volume of Fluid Model Setup and Interface Tracking

For printed electronics applications, CFD techniques, particularly the Volume of Fluid (VOF) approach implemented in Ansys Fluent, were essential for accurately resolving the ink-air interface during both droplet ejection and substrate spreading. These simulations enable the prediction of complex interfacial phenomena such as Marangoni-driven flows, tail formation, and contact line instabilities, all of which critically influence the dimensional accuracy and uniformity of printed lines [2], [8]. As demonstrated in Fig. 2, which presents force variation during ink expulsion alongside key deposition parameters [9], properly configured CFD frameworks with well-defined boundary conditions and validated material properties function as robust predictive tools for optimizing deposition performance.

In this study, the VOF method served as the primary multiphase modelling strategy for interface tracking throughout the deposition process, as shown in Fig. 3. The formulation employed a unified set of momentum equations across the computational domain, while interface fidelity was maintained using a volume fraction-based approach. ST effects at the fluid interface were incorporated through the continuum surface force (CSF) model to ensure accurate representation of capillary forces.

Interface reconstruction was carried out using the geometric reconstruction scheme (Geo Reconstruct) available within Fluent, which provides superior accuracy in estimating interface orientation and curvature when compared to donor-acceptor methods. This level of precision was particularly critical for capturing localized variations in contact line dynamics across substrates with differing surface energies. Pressure velocity coupling was resolved via the PISO (Pressure Implicit with Splitting of Operators) algorithm, chosen for its efficiency in handling transient multiphase flows. Momentum equations were discretized using a second-order upwind scheme, while the PRESTO! A scheme was adopted for pressure interpolation to improve gradient accuracy near the curved ink-air interface.

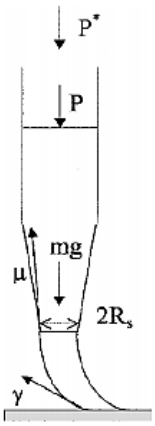

Fig. 2 *Force variation during ink expulsion, highlighting key deposition parameters [16]*

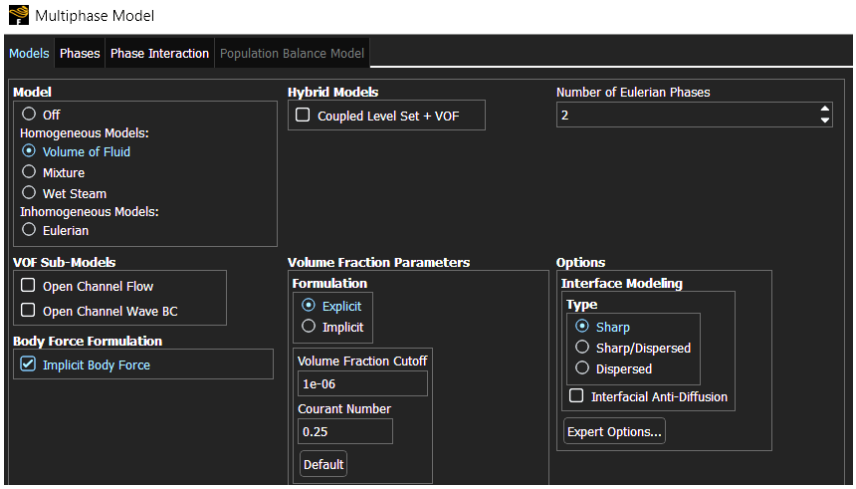

Fig. 3 *Represents the selection of VOF, implicit body force & volume fraction parameters*

2.5 Substrate Surface Energy Implementation

The thermodynamic principles governing liquid–solid wetting behavior are fundamentally linked to the system's tendency to minimize the total Gibbs free energy. The equilibrium configuration formed upon droplet–substrate contact represents the optimal balance between cohesive forces within the liquid phase and adhesive interactions at the solid–liquid boundary [6], [17]. This relationship is mathematically expressed by Young's equation (Equation 1), which defines the equilibrium contact angle θ as a function of the interfacial tensions. In practical deposition processes, dynamic wetting behavior often manifests through contact angle hysteresis, arising from differences between advancing and receding angles due to factors such as surface roughness, ink rheology, and chemical heterogeneity [7]. The present investigation applies static contact angle specifications as computational boundary conditions while acknowledging that transient wetting dynamics may contribute to discrepancies between numerical and experimental results. This approach is consistent with established practices that employ the VOF method for analyzing fundamental wetting interactions in conductive ink deposition [2], [5].

The deposition outcome strongly depends on the interplay between SSE and ST. These properties determine droplet spreading behaviour and ultimately govern the geometric precision of printed conductive patterns. Substrates exhibiting high SSE, such as glass or plasma-treated polymers, typically promote smaller equilibrium contact angles, enabling improved adhesion and uniform conductive pathways. Conversely, low-SSE materials, including untreated polymers or elastomeric substrates, often lead to insufficient spreading and the formation of irregular or discontinuous lines [6], [7].

In this study, SSE effects were incorporated by prescribing static contact angles at wall boundaries to represent various substrate materials. The simulation matrix included contact angle values ranging from 27.63° for high-energy ceramic substrates to 115.75° for low-energy silicone-based surfaces, thereby covering the range of wettability conditions typically encountered in printed electronics manufacturing. The equilibrium configuration of a droplet on a solid substrate is governed by the balance of interfacial tensions, described by Young's equation. The relevant interfacial energies are defined as, γSV represents the solid-vapor SSE, γSL denotes the solid-liquid interfacial energy, γLV corresponds to the liquid-vapor ST, and θ defines the equilibrium contact angle [6], [17]. These definitions are applied consistently throughout Eqs. (1) to (4).

$$\gamma SV = \gamma SL + \gamma LV \cos\theta \tag{1}$$

These contact angle specifications were enforced through the wall adhesion model in Ansys Fluent, which directly implements Young's equation (Eq. (2)).

$$cos\theta = \frac{\gamma SV - \gamma SL}{\gamma LV} \tag{2}$$

In Ansys Fluent simulations, θ critically influences the curvature near the contact line, directly impacting the accuracy of pattern fidelity predictions. To account for deviations from ideal surfaces, theoretical models such as the Wenzel and Cassie–Baxter frameworks provide additional interpretative capability. The Wenzel model incorporates roughness effects for chemically homogeneous substrates through the relationship (Equation 3):

$$cos\theta_W = r cos\theta_Y \tag{3}$$

where r represents the surface roughness factor quantifying the actual-to-projected surface area ratio [6]. For substrates exhibiting chemical heterogeneity or engineered surface patterns, the Cassie-Baxter model provides a more appropriate framework, expressing composite wettability (Eq. (4)).

$$cos\theta_{CB} = f_1 cos\theta_1 + f_2 cos\theta_2 \quad (4)$$

where f_1 and f_2 correspond to the fractional areas of distinct surface regions with respective contact angles. θ_1 and θ_2 [7]. These models are critical for interpreting differences between computational predictions and experimental observations, particularly for plasma-treated or microstructure substrates where microscale topographical and chemical features substantially influence droplet wetting behaviour and subsequent line formation.

2.6 Mesh Generation and Grid Independence Analysis

Computational mesh generation employed a structured grid approach within a cubic computational domain measuring 3×3×3 mm. This domain size provided sufficient space to capture the complete droplet trajectory and spreading behaviour while minimizing computational overhead. The computational mesh was generated using a structured hexahedral baseline grid with an initial element size of 0.04 mm, as shown in Fig. 4. This configuration resulted in approximately 421,875 elements for the overall domain. To improve accuracy near regions of high curvature and strong gradients, adaptive mesh refinement (AMR) was applied along the droplet trajectory and in the vicinity of the three-phase contact line at the substrate. The refinement strategy provided fine local resolution where it was most critical, while retaining coarser cells away from the interface to reduce computational cost. This approach ensured accurate prediction of spreading behaviour without requiring a uniformly fine grid across the entire domain.

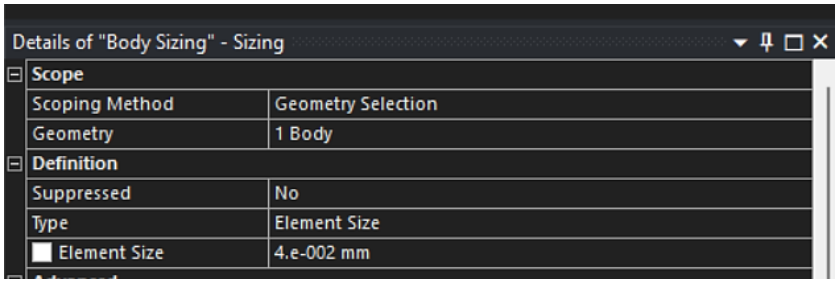

Fig. 4 *Represents the mesh element size selection*

Grid independence validation was performed by comparing baseline element sizes of 0.02 mm, 0.04 mm, and 0.06 mm prior to refinement. With AMR active, the effective local resolution near the droplet–substrate interface matched that of the 0.02 mm configuration, while the overall mesh size remained closer to the 0.04 mm baseline. Validation parameters including maximum spread diameter, equilibrium contact angle, and final line width showed less than 2% deviation from the finest mesh, confirming that the refinement strategy achieved equivalent accuracy while maintaining computational efficiency.

Mesh quality metrics were rigorously maintained throughout the domain, with orthogonality values exceeding 0.8 and aspect ratios remaining at unity for the structured hexahedral elements. The uniform mesh approach eliminated potential numerical artifacts associated with rapid grid transitions while ensuring consistent accuracy across the entire computational domain.

2.7 Parameters and Boundary Conditions

A controlled droplet deposition methodology was implemented to examine SSE effects on line width formation. Instead of modelling the entire syringe dispensing mechanism, a spherical droplet measuring 0.255 mm in radius (internal syringe tip radius) was initialized as specified in Fig. 5. The droplet was positioned 1 mm (deposition height) above the substrate under standard room temperature and pressure conditions. This approach offers several advantages. Complex fluid dynamics from nozzle exit flows were eliminated, yet the fundamental physics governing droplet impact and subsequent spreading remained intact. Starting with zero velocity, the droplet fell under gravity alone. Such a setup ensures reproducible conditions for studying how SSE affects deposition outcomes. Variable dispensing pressures and nozzle geometry complications were thus avoided.

Droplet dimensions were carefully chosen. The 0.255 mm radius represents volumes typical in precision dispensing while providing sufficient mesh resolution at the interface. At 25°C and 101.325 kPa, the gravitational acceleration of 9.81 m/s^2 acted on the droplet. Impact velocities achieved were characteristic of gentle deposition

processes used in printed electronics manufacturing. A 1 mm drop height served multiple purposes. This distance allowed droplets to form stable spherical shapes through ST before hitting the substrate. Simultaneously, impact velocity effects that might mask SSE influences were kept minimal. The height ensured ST and wetting forces would dominate over inertial effects during spreading.

The selection of 1 mm as the drop height aligns with empirical and theoretical observations on droplet impact dynamics. This distance maintains impact velocities in a range that avoids splashing, a phenomenon known to occur only beyond critical velocities significantly higher than those achieved at such low heights [18]. It also corresponds well to typical stand-off distances used in precision inkjet deposition, where 0.5-2 mm is considered optimal for maintaining stable trajectories and preventing mid-flight disturbances [19]. Furthermore, droplet spreading behaviour at this scale ensures that surface tension effects dominate over inertial forces, promoting uniform wetting and reducing the risk of rebound or irregular spreading, as established in studies of low-Weber-number regimes [20]. Thus, a 1 mm height effectively balances droplet stability, impact dynamics, and deposition accuracy, making it an optimal choice for this process.

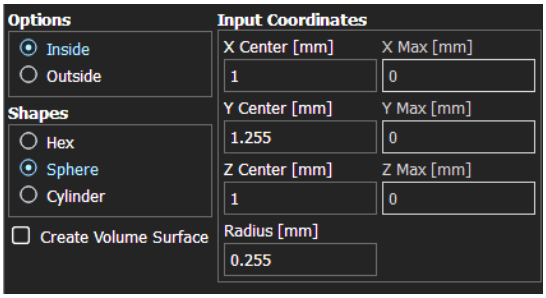

Fig. 5 *Droplet dimension & location input*

Dynamic time-stepping was implemented, with minimum intervals of 1 μs during critical phases such as impact and early spreading. Complete droplet evolution from release to equilibrium was captured, with simulations generally requiring 10-15 ms to achieve steady-state configurations, depending on substrate wettability characteristics. Earlier studies have demonstrated that CFD techniques can accurately reproduce droplet formation and motion when validated against experimental data, thereby supporting their application in analysing ink deposition behaviour [5]. The present analysis focuses on single-droplet spreading to isolate the influence of SSE and ST; however, future work will expand this framework to model continuous flow deposition at 0.1 m/s under defined curing conditions, thereby aligning more closely with experimental practice.

2.8 Enhanced Computational Model Integration

The computational framework incorporated an enhanced version of a predictive analytical model specifically modified to account for SSE and ST effects. This integration allowed direct comparison between empirical model predictions and detailed CFD results, facilitating model validation and refinement. The enhanced model [20] can be expressed as:

$$\alpha = \sqrt{\frac{2\pi {R_s}^4}{8\mu\left(tan\frac{\theta}{2}\right)v_0}\left(\frac{p}{hz}\right)} \tag{5}$$

The improved mathematical model introduces key parameters to enhance the prediction of conductive ink line width. Here, α represents the line width pattern, R_s corresponds to the nozzle tip radius, μ denotes ink viscosity, v_0 is the printing speed, θ signifies the contact angle of the deposited ink, p indicates the applied printing pressure, and hz defines the nozzle tip length. By explicitly integrating the contact angle (θ), a critical factor directly linked to SSE, the model achieves a more robust framework for line width estimation. This modification allows for the consideration of substrate-specific wetting behaviour, significantly improving the model's adaptability to diverse materials with varying SSE properties. As a result, the refined formulation delivers higher accuracy in predicting ink deposition dynamics, facilitating the optimization of printing parameters to achieve superior resolution and uniformity in conductive ink applications.

Line width predictions from the enhanced analytical model were calculated using substrate-specific contact angles and measured ST values. The model implementation considered the relationship between contact angle and SSE through established thermodynamic relationships, ensuring consistency between the simplified analytical approach and the comprehensive CFD analysis [21]. This dual-modelling approach provided both rapid

Int. Journal of Integrated Engineering Vol. 17 No. 8 (2025) p. 209-226

screening capabilities through the enhanced analytical model and detailed physical insights through full CFD simulation, supporting both fundamental understanding development and practical application optimization.

3. Results: Correlation of SSE and Formation of Line Width

The computational analysis demonstrated a direct relationship between SSE and conductive ink line width formation across seventeen substrate materials. The target line width of 0.8 mm was selected based on its significance in printed electronics applications, where precise line widths are required to maintain electrical resistance specifications and prevent short circuits between adjacent traces. Line width measurements ranged from 0.655 mm for silicone substrates (SSE = 16.49 mJ/m^2) to 1.23 mm for ceramic tile surfaces (SSE = 65.39 mJ/m^2), representing an 87.9% increase across the investigated SSE spectrum. Table 2 presents the comprehensive dataset obtained from Ansys Fluent simulations, encompassing SSE values, corresponding contact angles, and resulting line widths for each substrate material.

The data reveal distinct substrate clustering based on SSE characteristics. Engineering polymers (silicone through acrylic) clustered in the lower line width region (0.655-0.772 mm), while ceramic and specialty materials (porcelain through ceramic tile) occupied the higher line width range (0.875-1.23 mm). Fig. 6 illustrates the relationship between substrate surface energy (SSE), contact angle, and line width, highlighting the inverse correlation between SSE and contact angle, as well as the direct relationship between SSE and line width across all investigated substrate materials.

Table 2 *Results of SSE, contact angle, and line width*

S/No	Substrate	SSE (mJ/m^2)	Contact angle (°)	Line width (mm)
1	Silicone	16.49	115.75	0.655
2	Cardboard	16.80	115.23	0.657
3	Leather	18.14	111.95	0.666
4	PTFE	18.85	111.10	0.670
5	Rubber	24.87	100.08	0.675
6	PVC	24.95	99.93	0.676
7	Melamine coated surface	28.95	93.07	0.694
8	Polyethylene (PE)	30.30	90.80	0.728
9	Polypropylene (PP)	33.09	86.17	0.745
10	Acrylic	36.59	80.43	0.772
11	FR4	40.55	73.98	0.818
12	Glass	44.79	67.01	0.853
13	Porcelain	46.35	64.43	0.875
14	Unglazed ceramic tile	51.60	55.48	0.920
15	Glossy paper	53.36	52.35	0.951
16	Polyimide	59.24	41.27	1.069
17	Ceramic tile	65.39	27.63	1.230

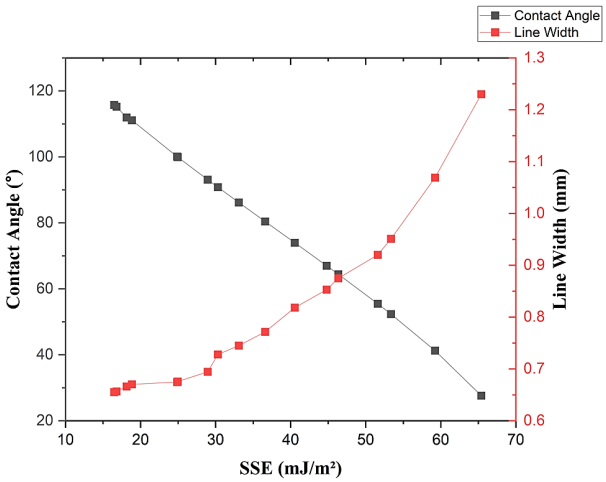

Fig. 6 *Relationship between substrate surface energy (SSE), contact angle, and line width, showing an inverse correlation between SSE and contact angle and a direct correlation between SSE and line width*

Analysis of the simulation results identified an optimal SSE range of 40-45 mJ/m^2 for achieving line widths closest to 0.8 mm. Within this range, two substrate materials demonstrated superior performance. FR4 substrate (40.55 mJ/m^2) produced a line width of 0.818 mm, representing a deviation of +2.3% from the target. Glass substrate (44.79 mJ/m^2) yielded a line width of 0.853 mm, showing a deviation of +6.6% from the target. Substrates with surface energies below 40 mJ/m^2 consistently underperformed, producing insufficient line widths. Acrylic (36.59 mJ/m^2) generated 0.772 mm width, falling 3.6% below the target. Conversely, materials exceeding 45 mJ/m^2 demonstrated overspreading behaviour, with porcelain (46.35 mJ/m^2) producing 0.875 mm width, representing 9.4% excess spreading.

The inverse correlation between SSE and contact angle measurements was confirmed across all seventeen materials. Contact angles decreased systematically from 115.75° for silicone substrates to 27.63° for ceramic tile surfaces, following a power law relationship with good correlation (R^2 = 0.983). For the target line width of 0.8 mm, corresponding contact angles ranged between 65-75°. This range aligns with moderate wetting conditions where ST forces balance spreading dynamics effectively. FR4 substrates exhibited a contact angle of 73.98°, while glass surfaces demonstrated 67.01°, both falling within the optimal wetting regime for controlled line formation. The contact angle range of 65-75° corresponds to the Wenzel wetting regime, where moderate wettability provides balanced spreading characteristics without excessive ink migration or insufficient substrate adhesion. Based on the deviation of line width from the 0.8 mm target, substrate materials were classified into three performance categories, as summarized in Table 3.

The classification into "optimal," "under-spread," and "over-spread" was grounded in tolerances commonly applied within printed electronics rather than chosen arbitrarily. International standards such as IEC 62899-202:2023 specify evaluation procedures for conductive inks, including surface tension, rheology, and resistivity, that directly link material behaviour to acceptable print performance [22]. Similarly, reliability studies have shown that line width deviations beyond approximately ±10% can lead to measurable increases in resistance variability and reduced adhesion under environmental stress conditions, particularly on low surface energy substrates [23]. Moreover, prior reviews of silver-based conductive inks emphasize that maintaining dimensional control within this window is critical for consistent electrical functionality in flexible and high-frequency applications [24]. Hence, the ±10% threshold adopted here reflects both published tolerance limits and practical constraints in manufacturing rather than an arbitrary classification.

Table 3 *Classification of substrate based on surface energy and line width deviation from the 0.8 mm target*

Performance category	Substrate	SSE (mJ/m^2)	Line width (mm)	Deviation from target (%)
Optimal performance (±10%)	FR4	40.55	0.818	+2.3
	Glass	44.79	0.853	+6.6
Under-spread (>10% below target)	Silicone	16.49	0.655	-18.1
	Cardboard	16.80	0.656	-17.9
	Leather	18.14	0.666	-16.7
Over-spread (>10% above target)	Ceramic tile	65.39	1.230	+53.8
	Polyimide	59.24	1.069	+33.6
	Glossy paper	53.36	0.951	+18.9

Fig. 7 presents an example of simulation results demonstrating the spreading behaviours across different SSE categories. The results show optimal line formation on FR4 substrate (Fig. 7(a)), insufficient spreading on silicone substrate (Fig. 7(b)), and excessive spreading on ceramic tile substrate (Fig. 7(c)). The enhanced model demonstrated improved predictive accuracy when validated against CFD simulation results, particularly within the optimal SSE range. For the target 0.8 mm line width, the model predicted optimal performance at 42 mJ/m^2 SSE, showing agreement within 5% of CFD predictions. Prediction errors remained below 6% within this range, confirming the model's suitability for engineering applications. Similar improvements were reported by Hern et al. [21], where the inclusion of SSE in a modified mathematical model reduced deposition errors from over 150% to below 16% across a wide variety of substrates. These results reinforce the value of incorporating substrate-specific characteristics into analytical frameworks to ensure robust and reliable predictions.

The simulation results demonstrate clear quantitative relationships between SSE, contact angle, and line width formation in conductive ink deposition. The identified optimal SSE range of 40-45 mJ/m^2 provides practical guidance for achieving target line widths in printed electronics applications, with FR4 and glass substrates demonstrating superior performance within ±7% of the 0.8 mm target. The enhanced model validation confirms

Int. Journal of Integrated Engineering Vol. 17 No. 8 (2025) p. 209-226

the reliability of predictive approaches for process optimization, particularly within the identified optimal SSE window.

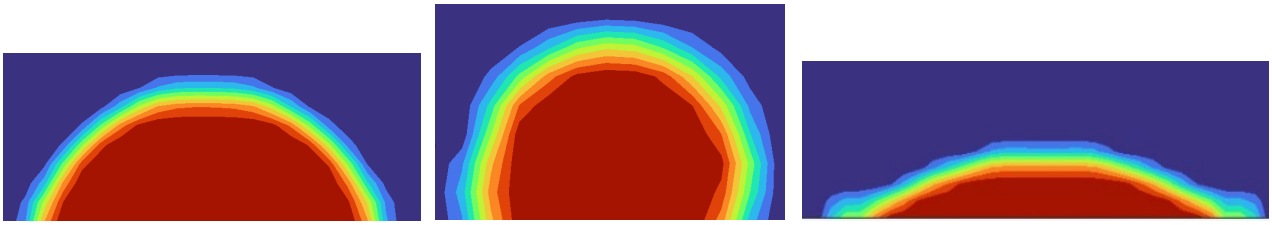

Fig. 7 *Simulation results based on SSE (a) FR4; (b) Silicone; (c) Ceramic tile*

4. Discussion

The growing use of conductive ink technologies in printed electronics, particularly for aerospace SHM systems, has increased the demand for improved deposition control and enhanced material compatibility. While advancements in ink chemistry and surface modification techniques have addressed certain manufacturing challenges, inconsistencies in deposition persist due to the complex interactions between SSE and ink properties. [2], [6]. Modern aerospace applications increasingly integrate printed SHM sensors within composite materials, where consistent ink patterns are critical for ensuring reliable operation under fluctuating thermal and mechanical conditions [9].

CFD has emerged as a vital tool for analysing spreading behaviour, line width evolution, and wetting interactions during ink deposition. Previous studies focusing on thick conductive pastes confirm that CFD simulations can accurately predict droplet–substrate interactions under various processing conditions [8], [9]. In line with these findings, the methodology adopted in this study employed a CFD model developed in Ansys Fluent to examine the influence of SSE on conductive ink spreading through a gravity-driven droplet simulation. This approach eliminates the complexity of modelling complete dispensing equipment while retaining the fundamental physics governing droplet impact and surface interaction, thereby providing an effective framework for linking theoretical principles to industrial requirements [2].

The performance of conductive inks is strongly influenced by their physicochemical properties, including viscosity, ST, and compatibility with the substrate. Even minor variations in these characteristics can markedly affect printed line uniformity, spreading behaviour, and ultimately the electrical functionality of the deposited features [2], [11]. Similarly, substrate attributes such as chemical composition, surface roughness, thermal conductivity, and porosity significantly impact the deposition quality. Smooth, dense surfaces like glass and aluminium generally promote uniform spreading and strong adhesion, whereas rough or porous materials frequently induce irregular deposition patterns and structural defects [6].

Substrates inherently exhibit different SSE values, which govern the interaction between the ink and the surface. Higher SSE promotes enhanced wetting, leading to greater droplet flattening, as illustrated in Fig. 6. This phenomenon occurs because surfaces with elevated surface energy form stronger molecular interactions with the liquid, effectively pulling the droplet outward to achieve a more stable configuration. Understanding these interfacial dynamics is fundamental to producing consistent and reliable printed structures.

The identification of an optimal SSE range of 40–45 mJ/m^2 offers manufacturers a practical guideline for substrate selection and surface treatment. This narrow range underscores the importance of precise control over surface characteristics, challenging conventional practices that rely on generic treatments. The observed 87.9% variation in line width (from 0.655 mm to 1.23 mm) across substrates demonstrates the critical role of SSE in transitioning from laboratory-scale prototypes to high-volume production.

Traditional manufacturing approaches tend to underestimate the interplay between surface chemistry and fluid dynamics. The present findings indicate that even substrates with comparable appearances can yield substantially different results. For instance, the contrast between FR4 substrates (0.8182 mm line width) and ceramic tiles (1.23 mm line width) exemplifies how SSE variations translate into significant process deviations. These sensitivities necessitate more advanced quality control measures than those currently employed.

The enhanced model confirmed the importance of integrating substrate-specific properties into computational frameworks. By incorporating SSE and ST effects, the model achieved a marked reduction in prediction error, maintaining accuracy within 6% in the optimal SSE range while still showing deviations at extreme conditions. This trend aligns with the experimental work of Moghtadernejad et al. [20], who demonstrated that error levels exceeding 150% with conventional approaches could be reduced to less than 16% once SSE effects were considered. Together, these findings underscore that predictive model in printed electronics must explicitly account for interfacial dynamics if they are to remain effective under industrial manufacturing conditions.

At very low SSE values, droplet dewetting and contact line instabilities likely dominate the spreading process, while at high SSE, rapid spreading may induce inertial effects and secondary flows that violate quasi-static assumptions. Furthermore, while the use of AMR improved interface resolution in the vicinity of the contact line, further refinement strategies, such as curvature-based refinement or dynamic refinement criteria, may offer additional improvements in capturing localized wetting instabilities without substantially increasing computational cost.

Finally, it is important to note that this study represents an initial stage of a broader investigation into printed electronics manufacturing parameters. The current results are limited to static deposition scenarios focusing on SSE effects on line width formation. Subsequent research will expand to include dynamic parameters such as deposition velocity and curing conditions, enabling the development of a comprehensive process optimization framework tailored for industrial-scale implementation.

5. Conclusions

This investigation demonstrated definitive quantitative relationships between SSE and conductive ink deposition behavior through an integrated computational approach. The analysis successfully addressed both primary research objectives: quantifying how SSE variations from 16.49 to 65.39 mJ/m^2 across seventeen substrate materials generate line width fluctuations of 87.9% and developing an enhanced Ansys Fluent simulation framework that delivered substantially improved predictive accuracy over traditional methods. Within the identified optimal SSE range of 40-45 mJ/m^2, errors remained below 6%, demonstrating the model's reliability for engineering applications. These improvements are consistent with the findings of Hern et al. [21] who showed that integrating SSE into predictive models reduced line width errors from more than 150% to below 16%. The corresponding contact angle window of 65-75° further highlights the precision required to transform current quality control approaches, offering manufacturers actionable guidelines for substrate selection and process optimization.

These results demonstrate that consistent deposition quality requires more sophisticated substrate property management than most manufacturing environments currently implement. The enhanced model validation confirms the industrial utility of incorporating substrate-specific SSE dynamics into predictive frameworks, demonstrating prediction errors below 6% within optimal conditions while revealing performance limitations at extreme surface energies that merit future investigation. The research implications extend across multiple industries confronting similar printed electronics integration challenges. Medical device manufacturers, automotive suppliers, and consumer electronics producers encounter comparable substrate-ink compatibility issues that these findings directly address. However, certain study limitations require acknowledgment, particularly the focus on room temperature conditions and single-droplet deposition events, whereas practical manufacturing involves continuous dispensing under fluctuating environmental conditions.

This work represents the first stage of a comprehensive investigation into printed electronics manufacturing parameters. Future phases will extend the present study by incorporating deposition velocity and curing parameters into a flowing deposition model rather than a single-droplet configuration, in order to better reflect real manufacturing conditions. A deposition velocity of 0.1 m/s has been selected to represent typical dispensing rates, where moderate inertia is expected to enhance spreading without inducing splashing. Curing effects will be examined using an oven temperature of 463.15 K together with a preheated substrate at 343.15 K. These conditions are expected to influence both line width stability and electrical performance: controlled curing should promote strong interfacial bonding and conductivity, while insufficient or excessive thermal exposure may result in adhesion loss or microstructural cracking. By integrating flow-driven deposition with thermal post-processing, the next stage of this research will provide a more comprehensive optimization framework for conductive ink printing under practical operating conditions. Several critical areas require further investigation to fully realize the commercial potential of these findings. Dynamic contact angle effects, neglected in the current study, likely influence deposition behaviour during the critical spreading phase. Understanding how contact angle hysteresis and dynamic wetting phenomena affect line formation could provide additional optimization opportunities.

The role of ink rheological properties beyond ST deserves systematic investigation. Many commercial conductive inks exhibit non-Newtonian behaviour, with viscosity varying under the shear conditions encountered during deposition. How these rheological complexities interact with SSE remains largely unexplored but could significantly influence practical applications. Multi-layer deposition strategies present another opportunity. Many electronic devices require multiple conductive layers with different electrical properties. Understanding how previous layers affect the SSE of subsequent depositions could enable more sophisticated device architectures and improved interlayer adhesion.

Environmental factors, including temperature, humidity, and atmospheric composition, influence both ink properties and substrate surface characteristics. Developing predictive models that account for these variables could extend the applicability of these findings to diverse manufacturing environments and seasonal variations. The enhanced understanding of substrate-ink interactions achieved through this work establishes a foundation

for advancing printed electronics manufacturing by bridging fundamental fluid dynamics with practical deposition challenges. This quantitative framework enables manufacturers to adopt predictive, optimized processes that consistently deliver superior results across diverse applications, supporting the continued evolution of flexible electronic systems.

Acknowledgement

This research was supported by Tier 1 (Vot J112) and GPPS (Vot Q581) by Universiti Tun Hussein Onn Malaysia (UTHM) and Fundamental Research Grant Scheme (FRGS/1/2023/TK10/UTHM/02/12) by the Ministry of Higher Education (MOHE).

Conflict of Interest

The authors declare that there is no conflict of interest regarding the publication of the paper.

Author Contribution

The authors are responsible for the study conception, research design, data collection, data analysis, result interpretation and manuscript drafting.

References

[1] Jessica Rocha Camargo, Luiz Otavio Orzari, Diele Aparecida Gouveia Araujo, Paulo Roberto de Oliveira, Cristiane Kalinke, Diego Pessoa Rocha, Andre Luiz dos Santos, Regina Massako Takeuchi, Rodrigo Alejandro Abarza Munoz, Juliano Alves Bonacin & Bruno Campos Janegitz (2021) Development of conductive inks for electrochemical sensors and biosensors, *Microchemical Journal,* 164, 105998, https://doi.org/10.1016/j.microc.2021.105998

[2] Mohamad Hannan Asyraf Hasnul Fauzi, Muhammad Najmi Zainal, Rd Khairilhijra Khirotdin & Wan Muhamad Syakir Wan Zaini (2021) A numerical and experimental investigation for deposition of conductive ink on multiple substrates with different surface energy and ink surface tension, *Research Progress in Mechanical and Manufacturing Engineering*, *5(1)*, 319-326.

[3] Y. Z. N. Htwe & Mariane Mariatti (2022) Printed graphene and hybrid conductive inks for flexible, stretchable, and wearable electronics: Progress, opportunities, and challenges, *Journal of Science: Advanced Materials and Devices, 7(2)*, 100435, https://doi.org/10.1016/j.jsamd.2022.100435

[4] Osman, Amr & Jian Lu (2023) 3D printing of polymer composites to fabricate wearable sensors: A comprehensive review, *Materials Science and Engineering: R: Reports,* 154, 100734, https://doi.org/10.1016/j.mser.2023.100734

[5] Gang Li, Tingting Liu, Xingzhi Xiao, Mingfei Gu & Wenhe Liao, Numerical simulations of droplet forming, breaking and depositing behaviors in high-viscosity paste jetting, *Journal of Manufacturing Processes, 78*, 172-182, https://doi.org/10.1016/j.jmapro.2022.03.047

[6] Mohamad Kannan Idris & Gerd Grau (2024) Dispense printing of silver flake inks on hydrophilic and hydrophobic surfaces, *Advanced Engineering Materials, 26(23)*, 2401302, https://doi.org/10.1002/adem.202401302

[7] Mendez-Rossal, Hector R. & Gernot M. Wallner (2019) Printability and properties of conductive inks on primer‐coated surfaces, *International Journal of Polymer Science,* 1, 3874181,

https://doi.org/10.1155/2019/3874181

[8] Liangkui Jiang, Li Yu, Pavithra Premaratne, Zhan Zhang & Hantang Qin (2021) CFD-based numerical modeling to predict the dimensions of printed droplets in electrohydrodynamic inkjet printing, *Journal of Manufacturing Processes, 66*, 125-132, https://doi.org/10.1016/j.jmapro.2021.04.003

[9] Bohan Li, Keming Ma, Shaowei Lu, Xingmin Liu, Ziang Ma, Lu Zhang, Xiaoqiang Wang & Sai Wang (2020) Structural health monitoring for polymer composites with surface printed MXene/ink sensitive sensors, *Applied Physics A, 126(10)*, 791, https://doi.org/10.1007/s00339-020-03979-4

[10] Xianfeng Wang, Xiaobo Liu, Guoping Ding, Xiaoyu Yan & Hao Cao (2022) Damage localization in holed carbon fiber composite laminates using FBG sensors based on back-propagation neural network, In *2022 5th International Conference on Data Science and Information Technology (DSIT)*, pp. 1-8. IEEE, https://doi.org/10.1109/DSIT55514.2022.9943829

[11] Ting Dong & Nam H. Kim (2018) Cost-effectiveness of structural health monitoring in fuselage maintenance of the civil aviation industry, *Aerospace,* 5(3), 87, https://doi.org/10.3390/aerospace5030087

[12] Zhaoyuan Wang, Jianming Yang & Frederick Stern (2008, January 7-10) *Comparison of particle level set and CLSVOF methods for interfacial flows*, In 46th AIAA Aerospace Sciences Meeting and Exhibit, Reno, Nevada. https://doi.org/10.2514/6.2008-530

[13] Shahab Mirjalili, Suhas S. Jain & Micheal Dodd (2017) Interface-capturing methods for two-phase flows: An overview and recent developments, *Center for Turbulence Research Annual Research Briefs*, 117-135,

[14] Jingfa Li, Dukui Zheng & Wei Zhang (2023) Advances of phase-field model in the numerical simulation of multiphase flows: A review, *Atmosphere, 14(8)*, 1311, https://doi.org/10.3390/atmos14081311

[15] Pooja Arya, Yanchen Wu, Fei Wang, Zhenwu Wang, Gabriel Cadilha Marques, Pavel A. Levkin, Britta Nestler & Jasmin Aghassi-Hagmann, Wetting behavior of inkjet-printed electronic inks on patterned substrates, *Langmuir, 40(10)*, 5162-5173, https://doi.org/10.1021/acs.langmuir.3c03297

[16] Giovanni Vozzi, A. Previti, D. De Rossi & A. R. T. I. Ahluwalia, (2002) Microsyringe-based deposition of two-dimensional and three-dimensional polymer scaffolds with a well-defined geometry for application to tissue engineering, *Tissue Engineering, 8(6)*,1089-1098, https://doi.org/10.1089/107632702320934182

[17] Lee, Hsien-Hsueh, Kan-Sen Chou, and Kuo-Cheng Huang, Inkjet printing of nanosized silver colloids, *Nanotechnology, 16(10)*, 2436, https://doi.org/10.1088/0957-4484/16/10/074

[18] T. C. De Goede, N. Laan, K. G. De Bruin & D. Bonn, Effect of wetting on drop splashing of Newtonian fluids and blood, *Langmuir*, *34(18)*, 5163-5168, https://doi.org/10.1021/acs.langmuir.7b03355

[19] Stephen D. Hoath, Wen-Kai Hsiao, Sungjune Jung, Graham D. Martin, Ian M. Hutchings, Neil F. Morrison & Oliver G. Harlen, Drop speeds from drop-on-demand ink-jet print heads, *Journal of Imaging Science and Technology, 57(1)*, https://doi.org/10.2352/J.ImagingSci.Technol.2013.57.1.010503

[20] Moghtadernejad Sara, Christian Lee & Mehdi Jadidi (2020) An introduction of droplet impact dynamics to engineering students, *Fluids*, *5(3)*, 107, https://doi.org/10.3390/fluids5030107

[21] L. Y. Hern, R. K. Khirotdin & N. Hassan (in press) Investigation on the deposition of conductive ink on multiple substrates with different substrate surface energy and ink surface tension properties, *International Journal of Integrated Engineering*.

[22] International Electrotechnical Commission (2023) Printed electronics – Part 202: Materials – Conductive ink, IEC 62899-202:2023, Geneva: IEC, https://www.iec.ch

[23] Riikka Mikkonen & Matti Mäntysalo (2018) Evaluation of screen-printed silver trace performance and long-term reliability against environmental stress on a low surface energy substrate, *Microelectronics Reliability*, 86, 54-65, https://doi.org/10.1016/j.microrel.2018.05.010

[24] Najwa Ibrahim, John O. Akindoyo & M. Mariatti (2022) Recent development in silver-based ink for flexible electronics, Journal *of Science: Advanced Materials and Devices,* 7(1), 100395, https://doi.org/10.1016/j.jsamd.2021.09.002